Research Square

Preprints are preliminary reports that have not undergone peer review.
They should not be considered conclusive, used to inform clinical practice,
or referenced by the media as validated information.

Delayed Cardiac Rupture 30 Days after Acute Myocardial Infarction in Oligosecretory AL Amyloidosis: A Case Report and Literature Review

Caixia Zhang[1]
Dingxi People's Hospital
Bo Zhang
Lanzhou Hospital of Traditional Chinese Medicine
Yiqun Li
Dingxi People's Hospital
Jielian Zheng
Dingxi People's Hospital
Longwei Gou
158316332@qq.com
Dingxi People's Hospital

Case Report

Keywords: Oligosecretory light-chain amyloidosis, cardiac amyloidosis, acute myocardial infarction, delayed cardiac rupture, left-ventricular pseudoaneurysm, nephrotic syndrome

Posted Date: November 25th, 2026

DOI: https://doi.org/10.21203/rs.3.rs-11355798/v1

License: This work is licensed under a Creative Commons Attribution 4.0 International License.
Read Full License

Additional Declarations: No competing interests reported.

Delayed Cardiac Rupture 30 Days after Acute Myocardial Infarction in Oligosecretory AL Amyloidosis: A Case Report and Literature Review

Caixia Zhang[1], Bo Zhang[2], Yiqun Li[3], Jielian Zheng[4], Longwei Gou[5*]

1. Department of Hematology, Dingxi People's Hospital, Dingxi 743000, Dingxi City, Gansu Province, China.

2. Department of Pediatrics, Lanzhou Hospital of Traditional Chinese Medicine, Lanzhou, 730050, Gansu Province, China.

3. Department of Nephrology, Dingxi People's Hospital, Dingxi 743000, Dingxi City, Gansu Province, China.

4. Department of Geriatric Medicine, Dingxi People's Hospital, Dingxi 743000, Dingxi City, Gansu Province, China.

5. Department of Critical Care Medicine, Dingxi People's Hospital, Dingxi 743000, Dingxi City, Gansu Province, China.

[*]Correspondence: Longwei Gou, Department of Critical Care Medicine, Dingxi People's Hospital, Dingxi 743000, Gansu, China.

Correspondence: Longwei Gou 158316332@qq.com.

Abstract

Background:

Amyloid light-chain amyloidosis is a rare clonal plasma cell disorder, and cardiac involvement is the leading cause of death. In the oligosecretory subtype, serum immunofixation electrophoresis is frequently negative, which renders misdiagnosis of nephrotic syndrome likely. Cardiac rupture is a fatal mechanical complication of acute myocardial infarction, characterized by a classic high-risk window within the first week after infarction; however, delayed cardiac rupture occurring 30 days after infarction has rarely been reported in systemic light-chain amyloidosis.

Case presentation:

A 61-year-old Han Chinese man presented with nephrotic syndrome. He had initially been misdiagnosed and treated with glucocorticoids, which resulted in bilateral osteonecrosis of the femoral head. Subsequent renal biopsy and bone marrow flow cytometry confirmed oligosecretory systemic light-chain amyloidosis involving the kidneys and heart. After four cycles of chemotherapy with bortezomib, cyclophosphamide, and dexamethasone, treatment was discontinued because of financial constraints. Approximately 3.5 years later, he developed acute myocardial infarction and underwent percutaneous coronary intervention. Thirty days after the infarction, he developed sudden cardiac rupture. Despite aggressive resuscitation, his haemodynamic status continued to deteriorate. His family elected to withdraw life-sustaining treatment, and the patient subsequently died.

Conclusions: Oligosecretory systemic light-chain amyloidosis presenting with nephrotic syndrome is frequently misdiagnosed. Myocardial amyloid deposition disrupts ventricular wall architecture and may lead to mechanical complications of

acute myocardial infarction beyond the classic time window. In patients with unexplained nephrotic syndrome, monoclonal light-chain testing and tissue biopsy should be performed as early as possible. Once the diagnosis is confirmed, standardized anti-plasma cell therapy should be maintained, and patients should be monitored for delayed cardiac rupture for a prolonged period after myocardial infarction.

Keywords: Oligosecretory light-chain amyloidosis; cardiac amyloidosis; acute myocardial infarction; delayed cardiac rupture; left-ventricular pseudoaneurysm; nephrotic syndrome

Introduction

Cardiac involvement in amyloid light-chain (AL) amyloidosis typically presents as restrictive cardiomyopathy. It is the leading cause of death in these patients and is associated with an extremely poor prognosis (1). Oligosecretory AL amyloidosis is especially susceptible to delayed diagnosis because of a low clonal plasma cell burden and negative routine serologic screening results (2); delayed diagnosis and treatment discontinuation may, in turn, lead to progressive amyloid deposition and ongoing myocardial structural damage (3). In this context, once acute myocardial infarction occurs, the increased myocardial fragility attributable to amyloid infiltration may extend the risk window for mechanical complications beyond the classic first week after infarction (4, 5). Currently, the clinical understanding of oligosecretory AL amyloidosis complicated by delayed cardiac rupture following acute myocardial

infarction remains limited (6). Here, we report one such case and discuss the diagnostic pitfalls and clinical implications in light of the current literature.

Case presentation

A 61-year-old Han Chinese male farmer with no significant medical history and an unremarkable family history was admitted to the Department of Nephrology at our hospital in December 2020; this patient presented with intermittent generalized oedema for more than 4 months, which had worsened over the preceding month. Four months prior to admission, the patient developed intermittent generalized oedema with no identifiable trigger, which was initially most prominent in the face and gradually extended to involve both lower extremities. The patient denied fever, gross haematuria, night sweats, or gastrointestinal symptoms. Urinalysis performed at an external hospital revealed 2+ proteinuria, and the patient was diagnosed with primary nephrotic syndrome. The patient was started on oral prednisone at a dosage of 60 mg daily, and the oedema improved; subsequently, the patient self-discontinued taking the medication. One month prior to admission, the oedema recurred and progressively worsened, manifesting as pitting oedema over the face and both lower extremities, accompanied by bilateral hip pain. He resumed 60 mg of prednisone daily, but his symptoms did not improve. He was admitted with a diagnosis of nephrotic syndrome. After the onset of the disease, the patient's urine output had decreased, but his mental status, appetite, sleep, and bowel habits remained essentially normal, and his body weight remained stable. On admission, his blood pressure was 114/87 mmHg,

with eyelid oedema and pitting oedema of both lower extremities. The initial laboratory findings on admission are summarized in Table 1.

Imaging

Transthoracic echocardiography revealed symmetric left ventricular wall thickening, with an interventricular septal thickness of 16 mm (reference range: 6–9 mm) and a left ventricular ejection fraction of 62%. Magnetic resonance imaging (MRI) of the hips revealed bilateral stage I osteonecrosis of the femoral head, which was attributed to glucocorticoid exposure.

Pathology

Bone marrow cytological examination revealed active marrow proliferation, with plasma cells accounting for less than 1% of the nucleated cells. Flow cytometry revealed approximately 0.77% monoclonal plasma cells with lambda (λ) light chain restriction. The overall plasma cell burden was markedly low, which is consistent with the oligosecretory subtype of AL amyloidosis. Histopathological examination of the renal biopsy revealed homogeneous, amorphous amyloid deposits within the glomerular mesangium on light microscopy. These deposits were accompanied by mesangial widening, segmental spicular changes in the glomerular basement membrane, and compression of the capillary loops. Minimal focal tubular atrophy was noted, with no significant interstitial fibrosis. Amyloid deposition was also observed in the small arterial walls, with luminal stenosis. Electron microscopy revealed numerous disorganized, unbranched, rigid fibrils measuring 8–12 nm in diameter within the glomerular basement membrane, mesangium, and small arterial walls. No

electron-dense deposits were identified. Immunofluorescence studies showed positive staining for the lambda (λ) light chain and negative staining for the kappa (κ) light chain and amyloid A (AA) protein. Special stains were positive for Congo red and oxidized Congo red. Based on these morphological and immunophenotypic findings, the pathological diagnosis was amyloid nephropathy (Figure 1).

Diagnosis and Initial Treatment of AL Amyloidosis

In January 2021, the patient was diagnosed with primary systemic AL amyloidosis (λ light-chain type, oligosecretory) according to the Chinese Expert Consensus on the Diagnosis and Treatment of Primary Light-Chain Amyloidosis (2016 Edition) (7). The disease was classified as Mayo 2004 stage II and Mayo 2012 stage II, with renal and cardiac involvement.

Between January and June 2021, the patient was treated with four 28-day cycles of bortezomib, cyclophosphamide, and dexamethasone (VCD) chemotherapy. Each cycle consisted of bortezomib 2 mg on Days 1, 8, 15, and 22; cyclophosphamide 0.5 g on Days 1, 8, 15, and 22; and dexamethasone 20 mg on Days 1–2, 8–9, 15–16, and 22–23. After four treatment cycles were completed, serum cardiac troponin I (cTnI) was 0.03 μg/L, and N-terminal pro-B-type natriuretic peptide (NT-proBNP) was 292 pg/mL, The 24-hour urinary protein was 3.04 g, and serum free κ and λ light chain concentrations were 7.66 mg/L and 27.76 mg/L, respectively. Echocardiography demonstrated an interventricular septal thickness of 12 mm and a left ventricular ejection fraction (LVEF) of 58%. In accordance with the response criteria of the

International Society of Amyloidosis (ISA)(8), haematologic response was defined as no response (NR)(9), whereas cardiac response met the criteria for cardiac complete response (CarCR)(10), and renal response met the criteria for renal partial response (renal PR)(11). Owing to financial constraints, the patient withdrew from treatment and was subsequently lost to follow-up for approximately 21 months.

In March 2023, the patient was readmitted for follow-up evaluation. Serum free κ light chain was 17.34 mg/L, while serum free λ light chain had risen to 99.21 mg/L; cTnI was 0.01 μg/L, NT-proBNP was 321 pg/mL, and 24-hour urinary protein was 3.69 g. Electrocardiography (ECG) showed sinus bradycardia (51 beats/min), left axis deviation, abnormal Q waves in the inferior leads, and poor R-wave progression in the precordial leads. Echocardiography revealed an interventricular septal thickness of 12 mm and an LVEF of 67%. Haematologic progression was confirmed. The cardiac response remained as CarCR, despite the presence of electrocardiographic abnormalities. No renal response or disease progression was observed. After one additional cycle of VCD chemotherapy, the patient was discharged, and treatment was interrupted once again.

Acute myocardial infarction and percutaneous coronary intervention

On November 28, 2024, the patient was admitted with a 2-day history of left upper quadrant abdominal pain in the absence of typical chest pain. ECG revealed abnormal Q waves in leads II, III, and aVF, accompanied by anterolateral ST-T changes. High-sensitivity cardiac troponin I (hs-cTnI) concentration was 8974.50 pg/mL, and the concentration of N-terminal pro-B-type natriuretic peptide (NT-proBNP) was

3532.22 pg/mL. Echocardiography demonstrated segmental wall motion abnormalities, increased myocardial wall thickness with a granular sparkling appearance, and a left ventricular ejection fraction (LVEF) of 43%. Cardiac magnetic resonance (CMR) imaging revealed left-ventricular myocardial and interventricular septal thickening, with patchy late gadolinium enhancement (LGE), consistent with cardiac amyloidosis (Figure 2). Coronary angiography showed total occlusion of the proximal left circumflex artery (LCx) and Thrombolysis in Myocardial Infarction (TIMI) 0 flow (Figure 3). After balloon predilation, the proximal-to-mid LCx showed a diffuse eccentric stenosis of approximately 30% with a superimposed thrombus, and antegrade flow was restored (TIMI 3). A distal LCx occlusion was then reopened by balloon angioplasty without significant residual stenosis. Balloon angioplasty was performed without stent implantation. The patient’s abdominal pain resolved after the procedure.

After the procedure, the patient was started on secondary preventive therapy for coronary artery disease, comprising aspirin 100 mg once daily, atorvastatin 20 mg once daily, clopidogrel 75 mg once daily, and dapagliflozin 10 mg once daily.

Delayed Cardiac Rupture and Clinical Outcomes

On December 28, 2024, 30 days after the index acute myocardial infarction, the patient presented with a 2-hour history of sudden-onset, severe abdominal pain radiating to the right shoulder. Physical examination on admission revealed a heart rate of 105 beats/min, distant heart sounds, and abdominal muscle rigidity, as well as

positive subxiphoid tenderness. An emergency ECG demonstrated abnormal Q waves in the inferior leads and low voltage in the limb leads. Laboratory tests revealed a haemoglobin (Hb) concentration of 103 g/L, a hs-cTnI concentration of 50.70 pg/mL, an NT-proBNP concentration of 9641.5 pg/mL, a D-dimer concentration of 12.47 μg/mL, and a fibrin degradation product (FDP) concentration of 67.7 μg/mL. Supportive fluid therapy was initiated after admission. One hour and ten minutes after admission, the patient's blood pressure decreased abruptly from 113/80 mmHg to 65/54 mmHg, prompting emergency transfer to the intensive care unit (ICU), where fluid resuscitation combined with intravenous norepinephrine infusion was administered to maintain circulatory perfusion, and blood component transfusion was also given. After transfer to the ICU, bedside echocardiography demonstrated thickening of the ventricular walls and the interventricular septum (15 mm). An endocardial echo discontinuity was identified in the mid-segment of the left ventricular posterior wall, associated with a saccular outpouching measuring approximately 23 mm × 14 mm, with a wide neck of approximately 11 mm. Colour Doppler imaging revealed bidirectional blood flow across the defect, consistent with a left ventricular pseudoaneurysm. Computed tomography (CT) demonstrated hepatic and splenic lesions, with amyloidosis as the leading diagnostic consideration, along with moderate pericardial effusion and a left ventricular pseudoaneurysm (Figure 4). Because of persistent hemodynamic instability, the norepinephrine infusion rate was escalated. Repeated bedside echocardiography showed increased pericardial effusion, and pericardiocentesis with indwelling catheter drainage was performed, yielding

continuous dark-red bloody fluid. These findings suggested hemopericardium secondary to rupture of the left ventricular pseudoaneurysm, a form of delayed cardiac rupture. Transfer to a higher-level hospital for surgical repair was recommended, but the patient's family declined and chose to discontinue treatment and discharge the patient. The patient died at home on the day of hospital discharge. The patient's clinical timeline is summarized in Table 2.

Discussion

Oligosecretory AL amyloidosis represents a distinct subtype of systemic light-chain amyloidosis. Owing to the extremely low clonal plasma cell burden and minimal monoclonal light-chain secretion, conventional serum immunofixation electrophoresis frequently yields negative results, leading to a high rate of underdiagnosis in routine clinical practice (12). This subtype typically presents with nephrotic syndrome as its sole initial manifestation and lacks the classic laboratory hallmarks of typical plasma cell disorders. In the absence of proactive screening combining serum-free light-chain assays with both serum and urine immunofixation electrophoresis, the condition is frequently misdiagnosed as primary nephrotic syndrome, leading to inappropriate glucocorticoid use, as well as delays in the diagnosis and treatment of the underlying disease (13). In the present case, serum immunofixation electrophoresis was negative, whereas urine immunofixation electrophoresis was positive for lambda light chains. Serum free lambda light chain was elevated at 43.20 mg/L (reference range, 5.71–26.30 mg/L), and the κ / λ ratio was reduced at 0.1637 (reference range, 0.26–1.65). Bone marrow flow cytometry also identified a monoclonal plasma cell population

(0.77%) with lambda light-chain restriction. Taken together, these findings were consistent with the oligosecretory subtype of AL amyloidosis. Despite the low clonal burden, ongoing light-chain production may result in progressive amyloid deposition in target organs, as exemplified by this patient.

Myocardial amyloid deposition represents a major determinant of long-term prognosis in patients with AL amyloidosis (14). Amyloid fibrils are progressively deposited in the myocardial interstitium, disrupting myocardial microarchitecture, reducing the mechanical stability of the ventricular wall, and increasing myocardial fragility, which collectively markedly impair myocardial repair capacity following myocardial infarction (5, 15). In typical acute myocardial infarction, free wall rupture typically occurs within the first week and is driven by rapid lysis of the necrotic myocardium. However, in the context of cardiac amyloidosis, the formation of stable scar tissue is impaired, and structurally vulnerable regions may persist within the infarcted myocardium, substantially prolonging the risk window for mechanical complications (16). Notably, in this patient, the index infarction arose from acute thrombotic occlusion of the left circumflex artery. After balloon predilation, the residual stenosis was approximately 30%, with a superimposed thrombus and restored TIMI 3 flow, suggesting a predominantly thrombotic rather than amyloid-related obstructive lesion. Even a relatively modest coronary occlusion can therefore be clinically significant, as amyloid infiltration had already compromised the structural integrity of the myocardium. Thirty days after the index myocardial infarction, the patient developed delayed cardiac rupture, which initially manifested with atypical abdominal pain

radiating to the right shoulder. This case highlights the heterogeneous presentation of myocardial infarction complications in the context of cardiac amyloidosis.

This case further highlights two key clinical challenges in the management of oligosecretory AL amyloidosis. First, the absence of early light-chain screening during the disease course led to inappropriate corticosteroid administration, culminating in permanent complications, including bilateral avascular necrosis of the femoral heads. Second, despite the absence of a partial haematologic response, cardiac and renal responses were documented. However, maintenance therapy was discontinued, leading to progressive elevation of serum free λ light-chain levels and progressive myocardial amyloid deposition. Consequently, cardiac damage progresses from subclinical structural abnormalities to impaired cardiac function and electrocardiographic abnormalities, ultimately culminating in delayed cardiac rupture following myocardial infarction. After four cycles of VCD therapy, the involved–uninvolved free light chain difference (dFLC) decreased by 44.4% with no haematologic response, whereas CarCR and renal PR were achieved. The dissociation between haematologic NR and organ responses indicates that organ responses are modulated by multiple factors, including volume status, renal function, and infectious status, and should thus be interpreted in the context of long-term follow-up (17, 18). This case demonstrates that the management of AL amyloidosis should target haematologic response, organ response, and long-term disease control. Sustained anti-plasma cell therapy is essential for halting progressive organ damage and preventing delayed fatal complications (19, 20).

Current literature indicates that cardiac rupture following myocardial infarction in patients with cardiac amyloidosis predominantly occurs within 6–10 days post-infarction and is most commonly associated with transthyretin amyloidosis (ATTR). Shirani et al. reported a case in which left ventricular free wall rupture occurred 6 days following acute myocardial infarction, with an autopsy confirming extensive myocardial amyloid deposition (21); Similarly, Pidello et al. described complete ventricular septal rupture 10 days after perioperative infarction in the setting of liver transplantation, with histopathology confirming intramural amyloid angiopathy (4); Additionally, Coisne et al. documented papillary muscle rupture secondary to obstructive intramural coronary amyloidosis (22). Although the AL amyloidosis cases reported by Tsai et al. and Soma et al. were complicated by myocardial infarction, no cardiac rupture was documented (6, 23). This case illustrates a rare presentation of oligosecretory AL amyloidosis complicated by delayed left ventricular free wall rupture 30 days following myocardial infarction. This not only expands the clinical spectrum of postinfarction mechanical complications in patients with cardiac amyloidosis but also suggests that the risk window for these complications may be prolonged, warranting extension of the monitoring window beyond the conventional 1-week timeframe in this high-risk population.

In the differential diagnostic workup, renal biopsy demonstrated λ light chain-restricted amyloid deposition. In conjunction with typical findings from cardiac magnetic resonance (CMR) imaging and echocardiography, the clinical picture was

highly consistent with AL amyloidosis. Given the patient's initial presentation of nephrotic syndrome and a negative family history of ATTR amyloidosis, ATTR amyloidosis was considered highly unlikely.

AL amyloidosis complicated by delayed cardiac rupture has an extremely poor prognosis. Once haemodynamic collapse and consumptive coagulopathy ensue, the likelihood of successful resuscitation is exceedingly low (14, 24). Surgical repair remains the only definitive treatment; however, most affected patients present with multiorgan amyloid involvement, poor baseline cardiac function, and coagulopathy, rendering surgery prohibitively high risk and unlikely to reverse systemic amyloid progression (25). Mechanical circulatory support may serve as a bridge to surgical repair, although its benefit remains limited in patients with end-stage amyloidosis (26, 27). In the present case, the patient's family declined surgical intervention, and mechanical circulatory support was not initiated. Therefore, the core preventive strategy for such life-threatening complications should prioritize early screening, accurate subtyping, and sustained treatment to halt progressive structural myocardial damage from the outset (28, 29).

Several limitations should be noted regarding this case. The diagnosis of cardiac amyloidosis was based on CMR and echocardiography, without histopathological confirmation via endomyocardial biopsy. In addition, neither autopsy nor transthyretin (TTR) gene testing was performed; thus, ATTR amyloidosis could not be definitively ruled out. Furthermore, the quantitative impact of treatment

interruption duration on myocardial involvement progression could not be reliably assessed.

Conclusions

Oligosecretory AL amyloidosis is highly prone to misdiagnosis and inappropriate management owing to its insidious clinical presentation and inherent screening challenges. Treatment interruption results in sustained accumulation of the myocardial amyloid burden, markedly prolonging the risk window for cardiac rupture following myocardial infarction and predisposing patients to fatal mechanical complications as late as 30 days after the index event. Clinically, patients with unexplained nephrotic syndrome should routinely undergo light-chain–related screening and biopsy. Once the diagnosis is confirmed, long-term standardized anti-plasma cell therapy should be maintained. For patients with myocardial infarction in the setting of cardiac amyloidosis, the conventional 1-week monitoring window should be extended, and prolonged surveillance for mechanical complications should be implemented.

List of abbreviations

AA: amyloid A

AL: amyloid light chain

ATTR: transthyretin amyloidosis

CarCR: cardiac complete response

CMR: cardiac magnetic resonance

CT: computed tomography

cTnI: cardiac troponin I

dFLC: difference between involved-uninvolved free light chains

ECG: electrocardiogram

FDP: fibrin degradation products

Hb: haemoglobin

hs-cTnI: high-sensitivity cardiac troponin I

ICU: intensive care unit

ISA: International Society of Amyloidosis

LCx: left circumflex artery

LGE: late gadolinium enhancement

LVEF: left ventricular ejection fraction

MRI: magnetic resonance imaging

NR: no response

NT-proBNP: N-terminal pro-B-type natriuretic peptide

PCI: percutaneous coronary intervention

PR: partial response

SD: stable disease

TIMI: Thrombolysis in Myocardial Infarction

VCD: bortezomib, cyclophosphamide, dexamethasone

Declarations

Ethics approval and consent to participate

This retrospective case report received approval from the Ethics Committee of Dingxi People's Hospital.

Consent for publication

Written informed consent was obtained from the patient’s next-of-kin for publication of this case report and any accompanying images. A copy of the written consent is available for review by the Editor-in-Chief of this journal.

Availability of data and materials

All the data generated or analysed during this study are included in this published article.

Competing interests

The authors have no conflicts of interest to disclose.

Funding

No funding was received for this work.

Authors' contributions

C.Z.: Conceived and designed the study, collected and analyzed the clinical and laboratory data, and drafted the initial manuscript.

B.Z.: Assisted in collecting clinical data and sorting out laboratory test results, and participated in the discussion of the treatment plan.

Y.L.: Performed the renal pathological examination and provided pathological images. Conducted a literature review and sorted out relevant academic materials, and participated in the revision of the discussion part.

J.Z .: Analysed the cardiac magnetic resonance and computed tomography images.

L.G.: Longwei Gou: Contributed to intensive care management and critically revised the manuscript. Supervised the study design and clinical diagnosis and treatment process, critically revised the manuscript for important intellectual content, finalized the manuscript, and is responsible for the integrity of the work.

All authors read and approved the final manuscript.

Acknowledgements

We thank the patient's family for consenting to publication and the pathology,

imaging, and ICU teams for their support.

References

1. Garcia-Pavia P, Rapezzi C, Adler Y, Arad M, Basso C, Brucato A, et al. Diagnosis and treatment of cardiac amyloidosis: a position statement of the ESC Working Group on Myocardial and Pericardial Diseases. Eur Heart J. 2021;42(16):1554-68.
2. Dispenzieri A, Kyle R, Merlini G, Miguel JS, Ludwig H, Hajek R, et al. International Myeloma Working Group guidelines for serum-free light chain analysis in multiple myeloma and related disorders. Leukemia. 2009;23(2):215-24.
3. Oubari S, Naser E, Papathanasiou M, Luedike P, Hagenacker T, Thimm A, et al. Impact of time to diagnosis on Mayo stages, treatment outcome, and survival in patients with AL amyloidosis and cardiac involvement. Eur J Haematol. 2021;107(4):449-57.
4. Pidello S, Simonato E, Orzan F, Frea S, Barreca A, Rinaldi M, et al. Interventricular Septal Rupture in a 62-Year-Old Man With Familial Amyloid Polyneuropathy. Tex Heart Inst J. 2020;47(4):302-5.
5. Cimini M, Hansmann UHE, Gonzalez C, Chesney AD, Truongcao MM, Gao E, et al. Podoplanin-positive cell-derived small extracellular vesicles contribute to cardiac amyloidosis after myocardial infarction. Cell Rep. 2025;44(3):115408.
6. Tsai SB, Seldin DC, Wu H, O'Hara C, Ruberg FL, Sanchorawala V. Myocardial infarction with "clean coronaries" caused by amyloid light-chain AL amyloidosis: a case report and literature review. Amyloid. 2011;18(3):160-4.
7. Hematology Oncology Committee of China Anti-Cancer Association, Leukemia & Lymphoma Group, Society of Hematology at Chinese Medical Association. [The consensus of the diagnosis and treatment of primary light chain amyloidosis in China (2016 version)]. Zhonghua Xue Ye Xue Za Zhi. 2016;37(9):742-746. Chinese. doi:10.3760/cma.j.issn.0253-2727.2016.09.003.
8. Gertz MA, Comenzo R, Falk RH, Fermand JP, Hazenberg BP, Hawkins PN, et al. Definition of organ involvement and treatment response in immunoglobulin light chain amyloidosis (AL): a consensus opinion from the 10th International Symposium

on Amyloid and Amyloidosis, Tours, France, 18-22 April 2004. Am J Hematol. 2005;79(4):319-28.
9. Palladini G, Dispenzieri A, Gertz MA, Kumar S, Wechalekar A, Hawkins PN, et al. New criteria for response to treatment in immunoglobulin light chain amyloidosis based on free light chain measurement and cardiac biomarkers: impact on survival outcomes. J Clin Oncol. 2012;30(36):4541-9.
10. Muchtar E, Dispenzieri A, Wisniowski B, Palladini G, Milani P, Merlini G, et al. Graded Cardiac Response Criteria for Patients With Systemic Light Chain Amyloidosis. J Clin Oncol. 2023;41(7):1393-403.
11. Muchtar E, Wisniowski B, Geyer S, Palladini G, Milani P, Merlini G, et al. Graded Organ Response and Progression Criteria for Kidney Immunoglobulin Light Chain Amyloidosis. JAMA Oncol. 2024;10(10):1362-9.
12. Kamarajan LP, Suman RR, Ranjan R, Kumar S, Krishna A, Mahto M. Unmasking amyloid light-chain amyloidosis through biochemical lens: diagnostic utility of urine immunofixation in serum-negative cases. Diagnosis (Berl). 2026;13(3):524-30.
13. Shafqat A, Elmaleh H, Mushtaq A, Firdous Z, Ashruf O, Mukhopadhyay D, et al. Renal AL Amyloidosis: Updates on Diagnosis, Staging, and Management. J Clin Med. 2024;13(6):1744.
14. Sanchorawala V. Systemic Light Chain Amyloidosis. N Engl J Med. 2024;390(24):2295-307.
15. Lavatelli F, Marchese L, Mangione PP, Raimondi S, Canetti D, Verona G, et al. Role of extracellular space and matrix remodeling in cardiac amyloidosis. Matrix Biol. 2025;140:100-12.
16. Chable-Guerrero FA, Romero-Zertuche D, Revilla-Monsalve C, Castrejón-Delgado L, Altamirano-Bustamante NF, Altamirano-Bustamante MM. Circulating Amyloid and Misfolded Biomarkers in Early Myocardial Injury: A Systematic Review and Epistemic Meta-Analysis. Int J Mol Sci. 2026;27(17):7956.
17. Staron A, Mendelson LM, Joshi T, Burke N, Sanchorawala V. Factors impeding organ recovery despite a deep haematological response in patients with systemic AL amyloidosis. Br J Haematol. 2024;205(6):2268-72.
18. Nuvolone M, Palladini G. Piecing together the intricate puzzle of organ recovery in AL amyloidosis. Br J Haematol. 2024;205(6):2119-21.
19. Wang W, Li J, Xu T, Yang Y, Yu C, Wang P, et al. Maintenance therapy promotes profound organ and haematologic response in light-chain amyloidosis patients not undergoing autologous stem cell transplantation. Ann Med. 2024;56(1):2418339.
20. Tan M, Chen Y, Ooi M, Mel S, Tan D, Soekojo C, et al. AL amyloidosis: Singapore Myeloma Study Group consensus guidelines on diagnosis, treatment and management. Ann Acad Med Singap. 2023;52(11):601-24.
21. Shirani J, Bonin MA, Gould N, Silver MA. Left ventricular free wall rupture following acute myocardial infarction and cardiac amyloid. Clin Cardiol. 1990;13(10):729-31.
22. Coisne D, Corbi P, Sosner P. Obstructive intramural coronary amyloidosis and papillary muscle rupture. Heart. 2003;89(2):E8.

23. Soma K, Takizawa M, Uozumi H, Kobayakawa N, Takemura T, Shiraishi J, et al. A Case of ST-elevated myocardial infarction resulting from obstructive intramural coronary amyloidosis. Int Heart J. 2010;51(2):134-6.
24. Kumar S, Dispenzieri A, Lacy MQ, Hayman SR, Buadi FK, Colby C, et al. Revised prognostic staging system for light chain amyloidosis incorporating cardiac biomarkers and serum free light chain measurements. J Clin Oncol. 2012;30(9):989-95.
25. Kumar S, Li D, Joseph D, Trachtenberg B. State-of-the-art review on management of end-stage heart failure in amyloidosis: transplant and beyond. Heart Fail Rev. 2022;27(5):1567-78.
26. Garg P, Alomari M, Wadiwala I, Lyle M, Pham S, Celik NB, et al. High profile transvalvular microaxial flow pump as a bridge to heart transplantation for amyloid cardiomyopathy: A case series. JHLT Open. 2025;10:100340.
27. Michelis KC, Zhong L, Tang WHW, Young JB, Peltz M, Drazner MH, et al. Durable Mechanical Circulatory Support in Patients With Amyloid Cardiomyopathy: Insights From INTERMACS. Circ Heart Fail. 2020;13(12):e007931.
28. Hollfoth V, Ali A, Bag E, Riemenschneider P, Mattern S, Luibrand J, et al. Accurate MS-Based Diagnostic Amyloid Typing Using Endogenously Normalized Protein Intensities in Formalin-Fixed Paraffin-Embedded Tissue. Mol Cell Proteomics. 2025;24(8):101040.
29. Castiglione V, Montuoro S, Orlando G, Aimo A, Vergaro G, Emdin M. Cardiac amyloidosis: Innovations in diagnosis and treatment. Eur Heart J Suppl. 2025;27(Suppl 1):i88-i97.

Table 1: Initial laboratory tests

Items	Result	Reference value
ESR (mm/h)	5	<15
WBC (× 10^9/L)	11.17	4.0-10.0
PLT (× 10^9/L)	143	100-300
Hb (g/L)	170	120-160
ALB (g/L)	21.80	35.00-50.00
ALT (U/L)	56.00	<40.00
AST (U/L)	25.20	<35.00
LDH (U/L)	543.40	120.00-220.00
ALP (U/L)	61.30	45.00-132.00
Ionized calcium (mmol/L)	2.16	2.00-2.80
Creatinine (μmol/L)	74.3	44.00-97.00
cTnI (μg/L)	0.01	<0.1
NT-proBNP (pg/mL)	4850	<125.00
24-h urine protein (g/24 h)	4.45	0.03-0.14
Autoantibody	Negative	Negative

APTT (Sec)	24.80	22.00-38.00
INR	0.82	0.80-1.30
Factor X activity (%)	76.3%	70.0-120.0
Serum protein electrophoresis	No monoclonal protein	
Serum immunofixation	No monoclonal protein	
Urine protein electrophoresis	No monoclonal protein	
Urine immunofixation	Free Lambda	
Gammopathy workup		
IgG (g/L)	2.09	8.00-16.00
IgA (g/L)	1.16	0.70-3.30
IgM (g/L)	0.76	0.50-2.20
Serum free light chains		
Kappa (mg/L)	7.07	3.30-19.40
Lambda (mg/L)	43.20	5.71-26.30
kappa/Lambda	0.1637	0.2600-1.6500

Abbreviations: ESR, erythrocyte sedimentation rate; WBC, white blood cell count; PLT, platelet count; Hb, haemoglobin; ALB, serum albumin; ALT, alanine aminotransferase; AST, aspartate aminotransferase; LDH, lactate dehydrogenase; ALP, alkaline phosphatase; cTnI, cardiac troponin I; NT-proBNP, N-terminal pro-B-type natriuretic peptide; APTT, activated partial thromboplastin time; INR, international normalized ratio.

Table 2 Patient timeline

Date	Clinical Event	Key Diagnostic & Therapeutic Interventions
December 2020	First presentation with generalized oedema; diagnosed with nephrotic syndrome	Prednisone therapy; positive urine immunofixation electrophoresis for λ light chain; bone marrow aspiration and renal biopsy
January 2021	Confirmed diagnosis of primary systemic AL amyloidosis (λ light-chain type, oligosecretory) with renal and cardiac involvement	Positive Congo red staining and λ-restricted amyloid deposition on renal biopsy
Jan 2021 – Jun 2021	Received 4 cycles of VCD chemotherapy regimen	bortezomib, cyclophosphamide, dexamethasone; haematologic no response (NR, 44.4% reduction in dFLC); cardiac complete response (CarCR); renal partial response (renal PR)
June 2021 – March 2023	Treatment discontinued; lost to follow-up for approximately 21 months	Disease progression with worsening cardiac involvement
March 2023	Readmission; 1 additional cycle of VCD regimen reinitiated	Haematologic progression confirmed with discordant organ responses; treatment interrupted again after discharge
28 November 2024	Admitted for left upper quadrant abdominal pain; diagnosed with acute myocardial infarction	Coronary angiography revealed LCx occlusion; PCI performed; CMR confirmed cardiac amyloidosis

28 December 2024	Sudden onset of severe abdominal pain and haemodynamic collapse	Bedside echocardiography and CT demonstrated a left ventricular pseudoaneurysm; pericardiocentesis yielded bloody pericardial fluid, consistent with cardiac rupture.
29 December 2024	Patient's family declined further treatment; discharged against medical advice	Died at home on the same day of discharge

Abbreviations: AL, amyloid light- chain; dFLC, difference between involved and uninvolved free light chains; VCD, bortezomib, cyclophosphamide, dexamethasone; PCI, percutaneous coronary intervention; LCx, left circumflex artery; CMR, cardiac magnetic resonance; CT, computed tomography; NR, no response; CarCR, cardiac complete response; renal PR, renal partial response.

A A1

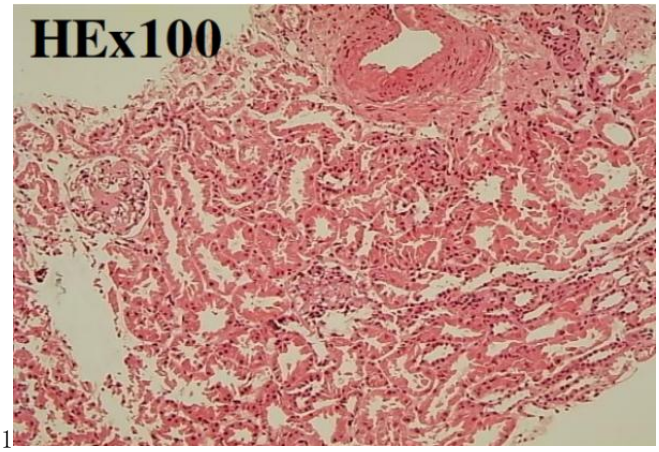

A2

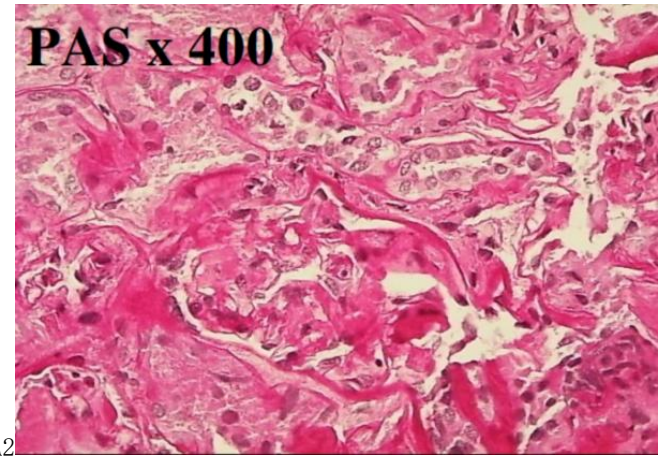

A3

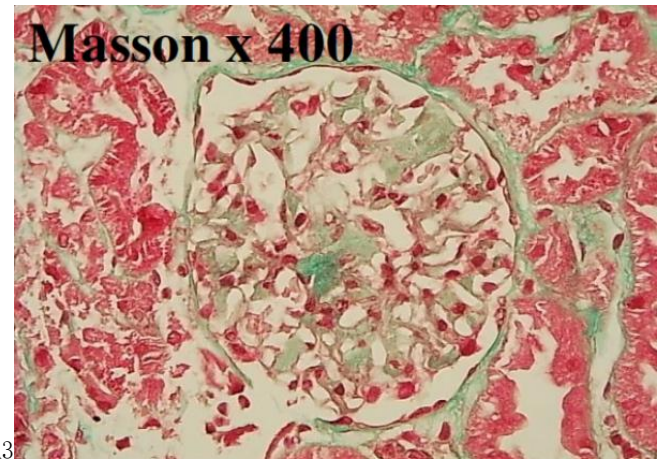

A4

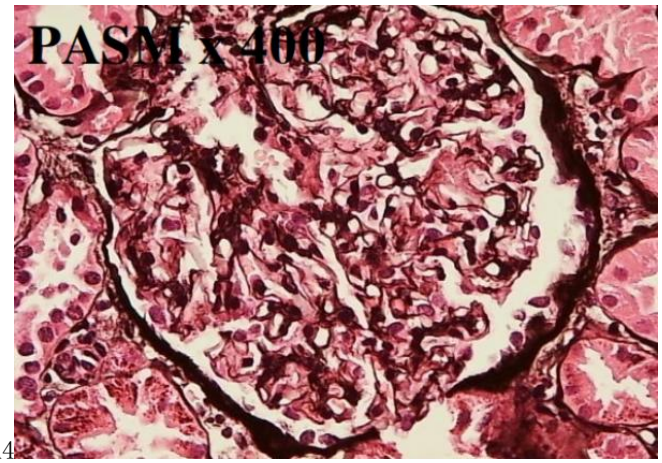

B B1

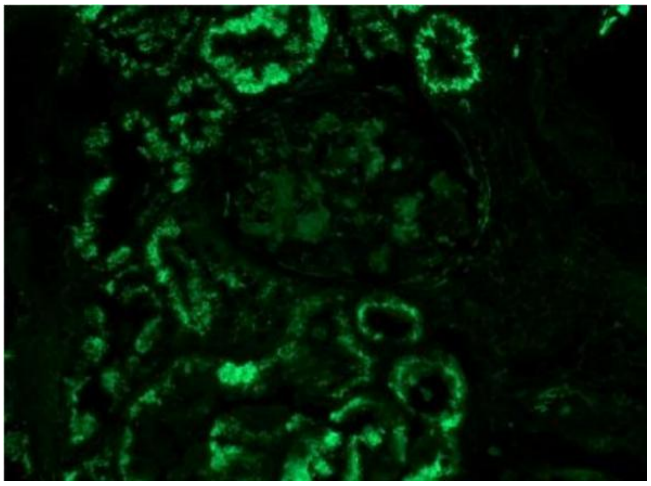

B2

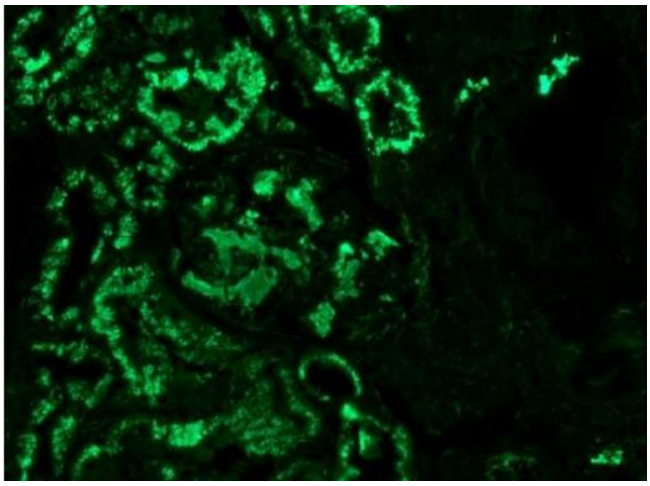

C C1

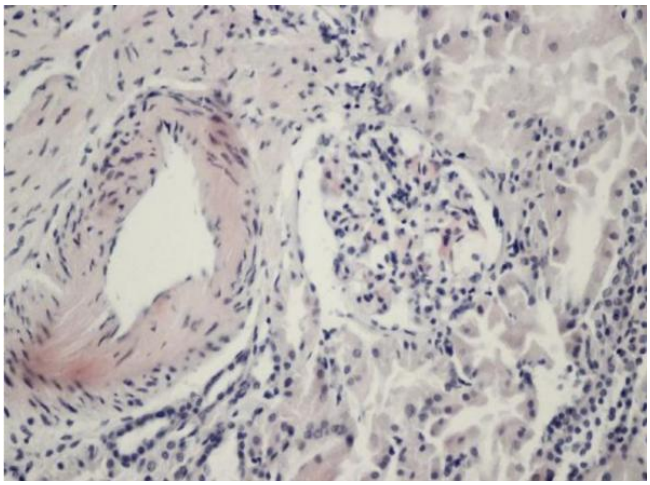

C2

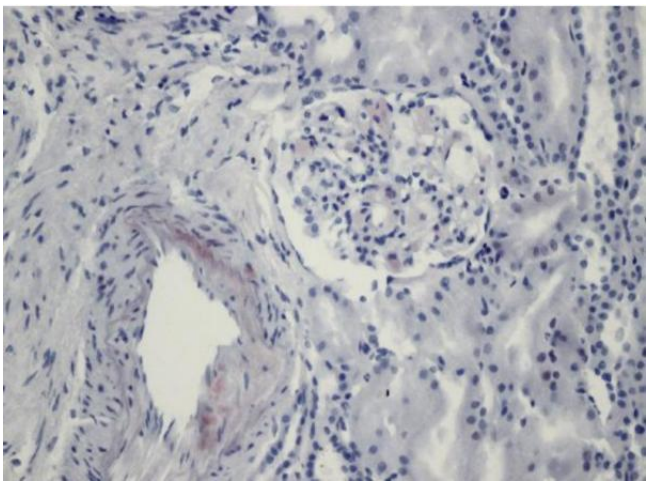

D D1

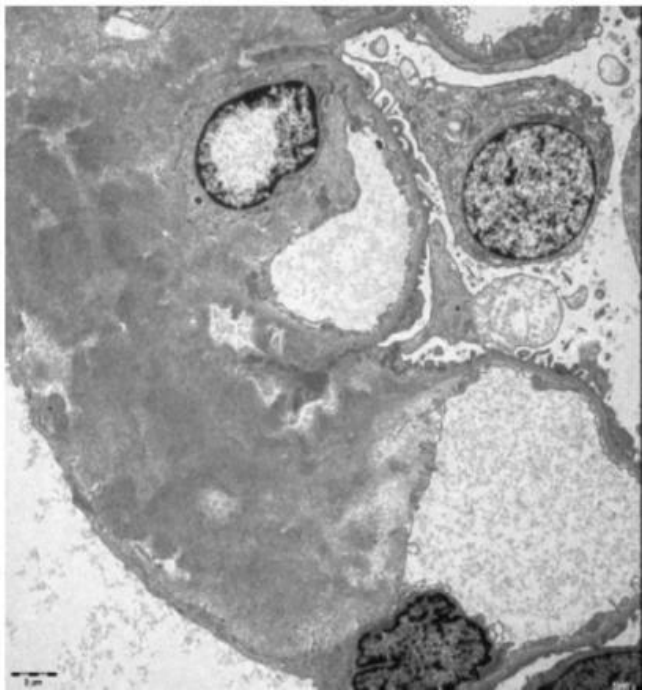

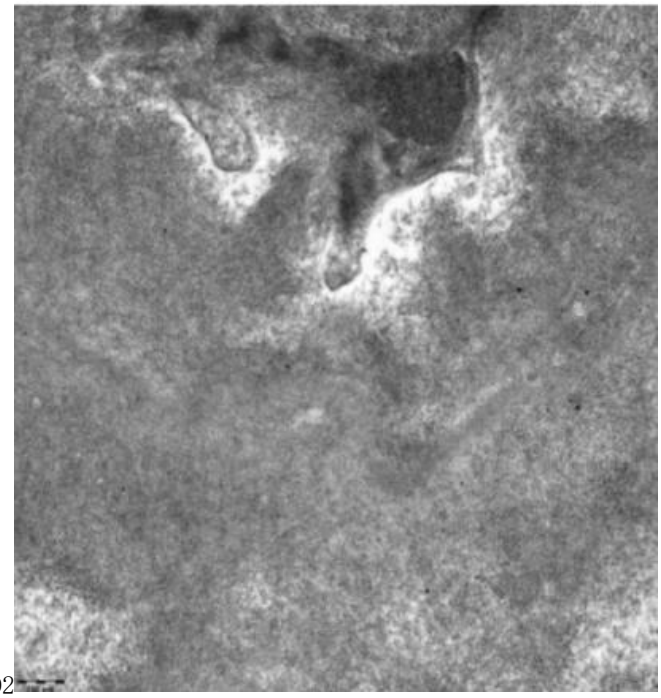

D2

D3 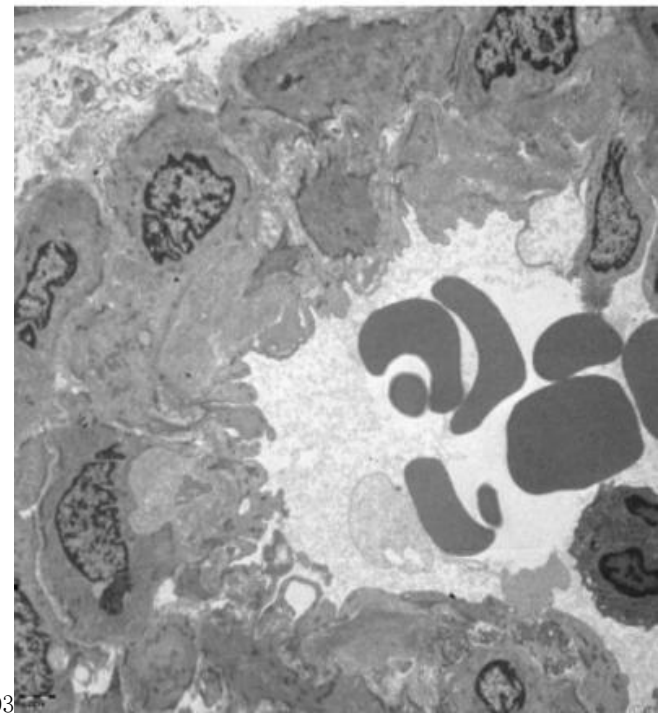

Figure 1. Pathological findings of renal biopsy. (A) Light microscopy images: A1, HE staining (100×); A2, PAS staining (400×); A3, PASM staining (400×); A4, Masson's trichrome staining (400×). Homogeneous eosinophilic amorphous deposits are seen within glomerular mesangial regions, accompanied by mesangial widening, segmental spicular changes in the glomerular basement membrane, and capillary-loop compression. Focal tubular atrophy and scattered interstitial inflammatory cell infiltration are present; small-arterial walls are thickened with luminal narrowing. (B) Immunofluorescence: negative for kappa light chain (B1) and positive for lambda light chain (B2), with mesangial and vascular wall deposits indicating lambda light-chain restriction. (C) Special staining: Positive Congo-red staining (C1) and positive oxidized Congo-red staining (C2). (D) Electron microscopy images: D1 (scale bar = 2 μm), D2 (scale bar = 500 nm), D3 (scale bar = 2 μm). Abundant unbranched rigid 8–12 nm fibrils are deposited in the mesangium, glomerular basement membrane and small-arterial walls; no electron-dense deposits.

A 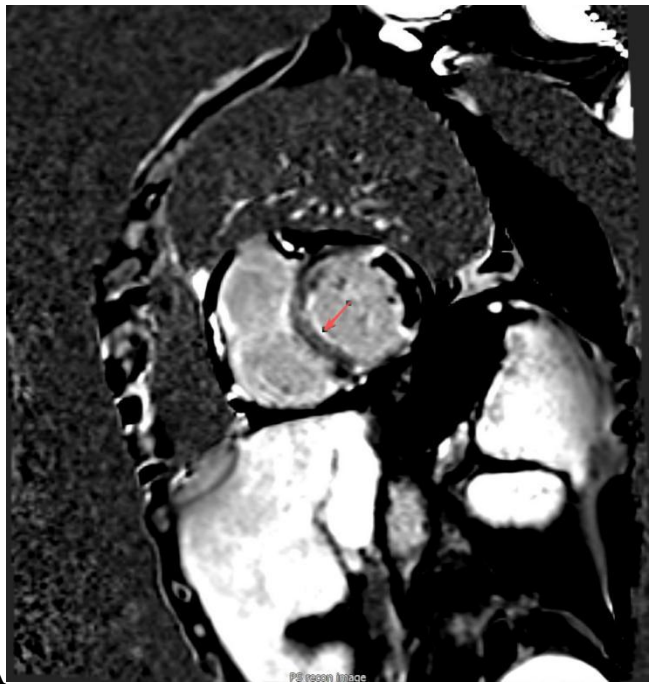

B



Figure 2. Cardiac magnetic resonance imaging. (A) Interventricular septal thickening. (B) Patchy myocardial late gadolinium enhancement.

A

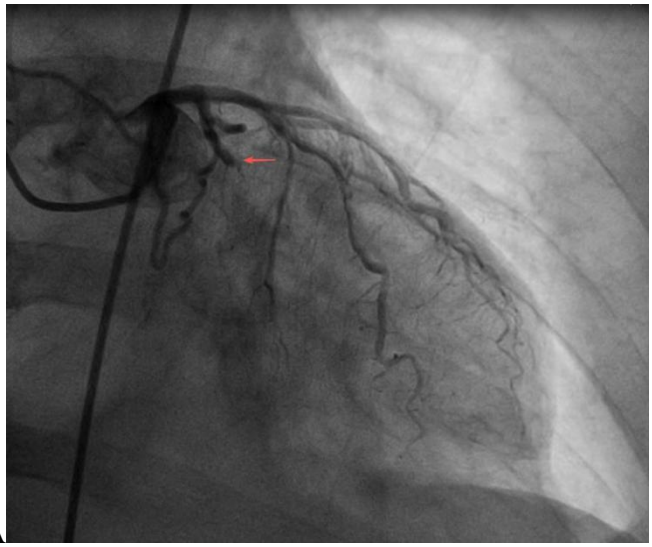

B

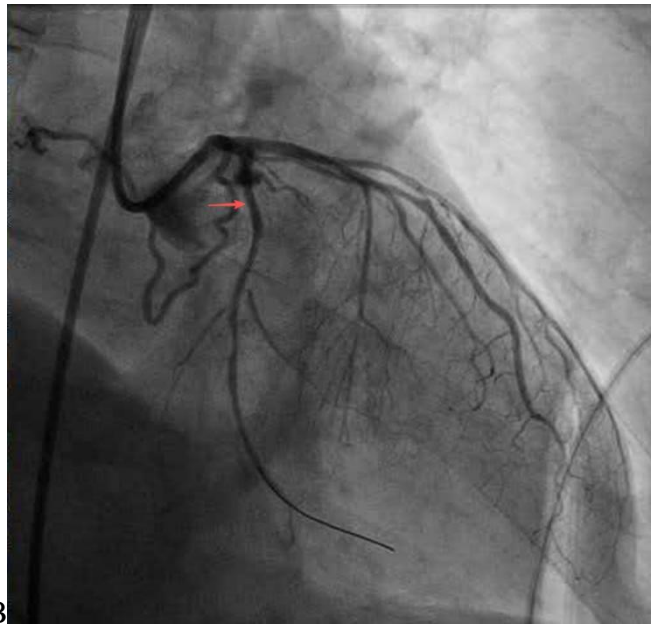

Figure 3. Coronary angiography. (A) Total occlusion of the proximal left circumflex artery (LCx) with TIMI 0 flow. (B) Restored antegrade flow (TIMI 3) after balloon angioplasty

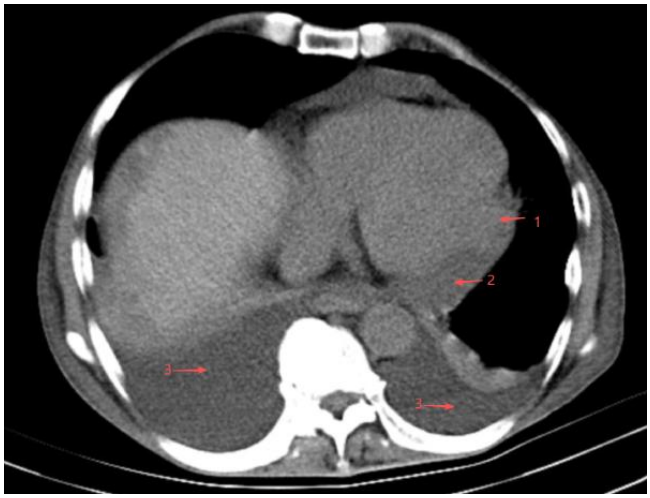

Figure 4. Computed tomography. Arrow 1: ruptured left- ventricular pseudoaneurysm; arrow 2: pericardial effusion; arrow 3: bilateral pleural effusion (two arrows labelled 3 indicate pleural effusion within the right and left thoracic cavities, respectively).

Supplementary Files

This is a list of supplementary files associated with this preprint. Click to download.

- CAREchecklist.pdf